6 Two Examples of Recent Crystal Development

Abstract. Two examples of recent scintillator development are given in this chapter. They have been chosen in two different areas of applications to illustrate the common strategies, but also the differences in the approach. Lead tungstate illustrates particularly well how large and very challenging fundamental research projects are instrumental in pushing the limits of detector performances to meet an ambitious scientific goal. On the other hand, Lutetium perovskite crystals, although developed up to mass scale production by an acamedic consortium (the Crystal Clear Collaboration), is a crystal to be used mainly in commercial systems like medical imaging devices. It is therefore constrained not only by technical considerations but also by a severe competition environment, as any new commercial product.

6.1 Example of Lead Tungstate Development for High Energy Physics Experiments

6.1.1 Introduction

High energy physics is a driving force in the development of new scintillators because of the high level of performance required in particle physics detectors and of the large volumes needed.

The first example of a well organized R&D effort for the development and mass production of scintillating crystals for a large high energy physics experiment is the L3 experiment [2] at the CERN Large Electron Positron collider in the 1980s. More than 12,000 bismuth germanate (BGO) crystals were produced at the Shanghai Institute of Ceramics (China) for this experiment (Fig. 6.1). Through the example of the CMS electromagnetic calorimeter being built at CERN in the frame of its Large Hadron Collider program this chapter describes the strategies developed for the R&D and the procurement of nearly 100 tons of lead tungstate scintillating crystals in a period of about 10 years. This project is now well under way as more than one half of the crystals have been produced so far (2005) and the detector is in its assembly phase.

The CMS experiment (Compact Muon Solenoid) [3] to be installed at the future Large Hadron Collider (LHC) at CERN has proposed the construction of a scintillator-based high-resolution homogeneous calorimeter, to meet the

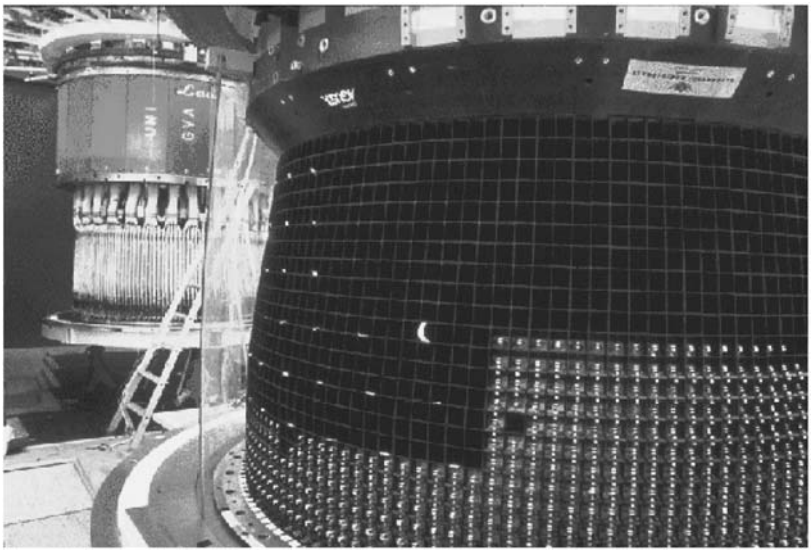

Fig. 6.1. BGO scintillation cells in the L3 Collaboration Electromagnetic calorimeter. An assembling phase

performance criteria for the discovery of an intermediate mass Higgs boson in its 2γ decay mode. The choice of lead tungstate crystals ($PbWO_4$) has been made in 1994 because of its high density, fast luminescence, and reasonable light yield and radiation resistance. It has also been decided to build a $PbWO_4$ electromagnetic calorimeter for the ALICE experiment [4] to take advantage of the very fine granularity allowed by the high density of this material, in order to resolve the high multiplicity events generated by heavy ions collisions at LHC. CMS will require 61,200 barrel crystals of trapezoidal shape divided into 17 types with average dimensions $(2.2 \times 2.2) \times (2.6 \times 2.6) \times 23$ cm^3 and 15,000 endcap crystal (one type) $(2.8 \times 2.8) \times (3 \times 3) \times 22\,\text{cm}^3$ for a total volume of $11\,\text{m}^3$ and a weight of 90 tons (Fig. 6.2).

The difficult physics constraints and harsh experimental conditions impose very tight specifications to modern detectors. The size of the experiments and the high quantitative demand allowed us to organize the R&D effort and production on a large scale (Table 6.1). This has been particularly illustrated by the work of the Crystal Clear Collaboration [1] which was able to create a multidisciplinary effort to make the best use of cross-fertilization between different categories of experts and industry to develop suitable scintillators at an industrial scale. In the case of the LHC program at CERN the possibility of making use of the large production infrastructure installed during the cold

Fig. 6.2. Some of the 80,000 CMS crystals on the automatic certification device

Table 6.1. Crystal calorimeters in the world

	Crystal Ball	Cleo II	L3	Babar	Belle LoI	L* EoI	GEM EoI	L3P	ALICE	CMS
Where	SPEAR	CESR	LEP	SLAC	KEK	SSC	SSC	LHC	LHC	LHC
When	1972	Late	1980s	1999					2007	2007
Beam	e^+e^-	e^+e^-	e^+e^-	e^+e^-	e^+e^-	pp	pp	pp	ion–ion	pp
Energy (Gev)	4	6	100	$9+3.1$	$8+3.5$	20	8,000	8,000	5.500	7,000
Crystal	NaI:Tl	CsI:Tl	BGO	CsI:Tl	CsI:Tl	BaF_2	BaF_2	CeF_3	$PbWO_4$	$PbWO_4$
Number (k)	0.7	7.8	11.4	6.8	8.8	26	45	100	18	77
Length (X_0)	16	16	21.5	16	16	24.5	25	25	22	25
Photodetector	PMT	SiPD	SiPD	SiPD	SiPD	V4T	SiPD	VPD	SiPD	APD/V3T
B(T)	0	1.5	0.5	1	1	0.75	4	1	0.5	4
f_{BC} (MHz)	1.3	2.8	0.091	2.38	10	60	67	67	8	40

war in former Soviet Union has been a key to the success. This has motivated the collaboration of physicists with the International Science and Technology Center (ISTC) [5] for the conversion of the Bogoroditsk Techno-Chemical Plant in Russia for the production of a large fraction >90% of the 80,000 lead tungstate crystals for the CMS experiment at CERN. The rest of the crystals are produced by the Shanghai Institute of Ceramics in China.

6.1.2 The Conditions of Scintillator Development for High Energy Physics (HEP)

The context of scintillator development for HEP is rather difficult. The market cannot be stabilized because of the rapidly evolving demand at each generation of experiment. The very large size of the projects imposes a strong effort of development and production in a relatively short period of time. Unfortunately the benefit of these efforts is very often lost if the next experiment requires another scintillator with improved performances. For a long time NaI(Tl) was the only candidate because the most important parameter was a high light yield to be able to read out the signals from low energy particles with standard electronics. Then, the increasing size of the experiments and the necessity of having a good granularity of the detectors opened the research toward higher density materials. That was the era of BGO with a very high density of 7.13 but a rather moderate light yield and CsI with a smaller density of 4.51 but a much higher light yield, which seems to have been a good compromise, as it is the only scintillator to have been used in at least five large size detectors so far. Unfortunately the hunt for very rare events imposed to build accelerators of higher luminosity, putting new constraints for short decay time of the scintillators. The requirements for high density have been further increased, whereas the one for high light yields has been somehow reduced because of the increased energy of incoming particles and of the emergence of new type of photodetectors such as avalanche photodiodes. These new requirements triggered a strong R&D effort on BaF_2, CeF_3, and $PbWO_4$.

Another difficulty for this activity is the complexity of the decision mechanisms in HEP. As new technologies are needed for every new generation of experiment, an important R&D effort has to be made for a proof of feasibility and a good understanding of cost issues, before any approval can be made. This takes usually several years during which no firm commitments can be made and some conditions can change. At least two difficult cases were experienced in the recent past:

- The large effort of several years for the development of large size radiation hard blocks of BaF_2 crystals was suddenly stopped by the decision to stop the SSC program in the USA.
- Similarly, the spectacular developments of avalanche photodiodes have led the CMS collaboration to finally prefer lead tungstate crystals with a lower light yield but higher density, to the higher light yield cerium fluoride CeF_3, in order to build a more compact and less expensive detector.

The uncertainty of future markets for these new scintillators is another problem for the crystal producers. At least in the first phases of the development the prospects for other applications than physics experiments are not well known. Although the situation has been rather good for BGO in the scientific, industrial, and medical domains, reasonably good for CsI with

several physics experiments and some commercial applications, it is still very unclear for BaF_2, CeF_3, and $PbWO_4$.

On top of these difficulties, the more and more severe budgetary constraints impose strong limits on the production costs of the scintillators which are only partially compensated by the financial support during the R&D phase.

Keeping in mind all these difficulties, a proper strategy has been set up for the development and production of the large quantity of lead tungstate crystals of the CMS electromagnetic calorimeter.

6.1.3 Strategy for the CMS Calorimeter

6.1.3.1 General Considerations

The first and probably most important action in the beginning of such a challenging project is to clearly define the objectives. This includes a strict definition of a list of realistic specifications to be reached by the crystal, in order to guarantee the physics performance of the detector without overdesigning. The understanding of the cost-driving factors and the study of the methods to reduce their impact on the final cost has to be included in the R&D program at the same level as the fight for improved technical parameters. Finally, the preparation of the production infrastructure must be included in the overall program with a detailed analysis of all the production aspects: procurement of raw materials, equipment, manpower, and safety. In the case of CMS a program has been set up in three phases with 3 years' R&D, 2 years' preproduction, and about 5 years' production periods.

A proper funding must be defined for each phase in full agreement with the crystal producers. It is important that the losses are minimized in the case of a modification or even a stop at any stage of the program. For the first time in the history of high energy physics, CMS has organized a well-defined support during the R&D and the preproduction phase funded by CERN with the help of the International Science and Technology Center (ISTC) in Russia. ISTC is an intergovernmental organization to bridge between Russian institutes and the world market and to promote their conversion from military to civil applications. This long-term effort associated with a nonnegligible risk must be shared with well-selected industrial partners. The possibility of making use of the large production infrastructure installed during the cold war for the growth of nonlinear crystals for military applications has played an important role in the selection of the Bogoroditsk Techno-Chemical Plant (BTCP) in Russia.

The traditional client–producer relationship must be replaced by a more effective spirit of collaboration. A mutual understanding of the different constraints on both sides has to be built in the necessary respect of a certain level of confidentiality to protect the long-term interests of the producers. This sociological aspect is very important and although it takes generally

several years to be fully integrated, it contributes to a large extent to the success of the operation. Such challenging projects cannot be successfully realized without solving the difficult equation of maximization of happiness on both sides: best performances for lowest cost on the client side, versus best profit and possibility of attracting other clients on the producer side.

6.1.3.2 Organization of the R&D

An important characteristic in the field of material science is that it requires a multidisciplinary approach. The users (in our case high energy physicists) define a set of desired performances which determine the goal to be reached. The crystal producers bring the technology and their experience in organizing mass production with maximum yield and optimized cost. A group of experts are also needed in different fields such as solid state physics, spectroscopy, chemistry, and trace element analysis, to help producers to reach the specifications set by the users. Some of the required expertise may exist in the production centers, but in most of the cases one has to open the collaboration to outside laboratories. One difficulty is to select these groups not only for their expertise but also for their ability to understand the specific spirit of their contribution. They have on the one hand to understand the user's requirements and on the other hand to help solving problems in an industrial context and not only for their academic interest. This is a long-term work, and the experience gained in previous large projects as well as R&D efforts in the frame of officially supported groups such as the Crystal Clear collaboration at CERN [1] plays a crucial role in organizing these contacts.

Another problem comes from the difficulty of the measurements in the field of material sciences, which require very often heavy equipment with scheduled access spread in different parts of the world. This is the case for synchrotron radiation sources, radiation facilities, EPR systems, and to a lesser extent for thermo-luminescence and elaborated spectroscopic devices. The time needed to perform and analyze the results of the experiments is long. This is why a specific organization had to be made in order to reduce the feedback loop with the producer. For each problem (radiation hardness), or quantity to be improved (light yield), experts are asked to propose a few tests to identify the parameters involved in this problem. Once these parameters are known, they are systematically scanned by the producer in order to find the best optimization. At this stage, a two-level feedback loop is organized, one with a few simple tests made in the vicinity of the production center to allow quick reactions, and another one with more indepth studies in specialized laboratories for a full control and understanding of the process. Once a significant improvement seems to have been made, it has to be confirmed on a statistical basis on a set of at least 10 full-size crystals in the conditions of mass production. This approach reduces as much as possible the time needed to solve a problem. However, one has to count about 1 year for each important step in the development of a new material. This is the time

it took the CMS collaboration to grow crystals of the required dimensions in 1994, to suppress slow components at the end of 1995, and more recently to make significant progress in radiation hardness of lead tungstate crystals [6].

6.1.3.3 Cost Optimization

One important aspect of these developments is the cost optimization. All the R&D effort must be driven by cost considerations. It is not sufficient to solve a problem with nonaffordable solutions. This is why the R&D as well as the production strategy is developed as a function of the existing infrastructure in the production centers. It is cheaper to extract specified impurities in 5N raw materials than to have to buy 6N pure components. Optimizing the orientation of the crystal and the annealing procedure is certainly cheaper than developing specific machines for cutting fragile crystals. The maximization of the yields at each stage of the production is one of the key objectives of the R&D.

As potential future markets are uncertain, the production infrastructure has to be organized as much as possible with R&D funds, in order to not impinge too much on the production cost of the crystals. This is also the role of the R&D to develop production technologies as simple as possible, minimizing the power consumption, and with a high degree of automatization in order to reduce manpower costs.

6.1.4 Progress on Lead Tungstate

This systematic approach has been followed for the development of Lead Tungstate crystals for the CMS experiment at CERN.

The very specific requirements of the scintillating crystals for the Electromagnetic Calorimeter at the CERN Large Hadron Collider CMS experiment have been the subject of intensive research and development for about ten years. At the start of these studies it was by no means clear that the very high purity of raw material, nor the special and harsh requirements regarding the radiation hardness of these crystals could be met at all. None of the most experienced manufacturers in the field was at that time anywhere close to being able to deliver the quality of crystals needed. An intensive long-term R&D effort was therefore undertaken by a scientific research consortium including the international CRYSTAL CLEAR Collaboration [1], members of the CERN-CMS experiment, the Institute of Nuclear Problems from Minsk and the Bogoroditsk Techno-Chemical Plant from Russia. It operated under the umbrella and with the active help of the ISTC and with generous financial support from the European Union as one of the major founding Parties to the ISTC Programs. A large development effort has also been undertaken with the Shanghai Institute of Ceramics in China.

Systematic studies from this large community as well as from others groups who jointed the PWO R&D effort at different stages have led to

several important results. They allowed to improve significantly the quality of the crystals and to prepare the final specifications for the production of nearly 80,000 PWO crystals, which have to remain stable and well calibrated under the harsh running conditions of the LHC. Most of these results have been obtained in a relatively short period of time (3 to 4 years). The most significant ones are listed below:

6.1.4.1 Crystal Growth Orientation

At the first stage of the R&D the crystal growth conditions have been optimized. The natural direction of the crystal growth is along the c-crystallographic axis. However the bi-refrigency of the crystal is a critical issue for obtaining a uniform light yield in the $25X_0$ long scintillation elements. It was found that under specific conditions the crystals could be successfully grown along the a-crystallographic axis. Moreover this crystal growth orientation produced an elliptic cross-section of the ingot. which improved the crystal/ingot volume ratio at the machining stage. With this approach, and after a long optimization of all the growth parameters the yield of barrel and endcap growth and annealing could reach the impressive value of 95%.

6.1.4.2 Improvement of the Crystal Transparency

One of the problems which has been successfully resolved is the suppression of the yellow color of lead tungstate crystals. This is a common problem for the tungstate and molybdate crystal families, which was successfully resolved for the first time. This yellow color results from two wide absorption bands with maxima near 420 and 370 nm. It was found that the origin of the 420 nm band is due to a charge transfer transition on a trivalent lead ion state about 1 eV below the bottom of the conduction band. Changing the atmosphere of the crystal growth to a neutral gas purified from oxygen and water immediately suppressed the coloration and resulted in the production of very transparent lead tungstate crystals. This important progress is illustrated in Fig. 6.3. The second band at 350–370 nm is usually present in crystals grown in not optimal conditions. The intensity of this band is well correlated with the intensity of radiation induced absorption in the scintillation region. This band is annealed in air at a temperature close to the melting point. The center responsible for this band is converted under UV irradiation to another center with maximum of absorption near 410 nm. The origin of this center has been identified as an irregular anionic tungstate complex distorted by a Frenkel defect. Following this interpretation both the 420 and the 370 nm bands have been simultaneously suppressed by trivalent rare earth doping of the crystals. The resulting improvement of the crystal transparency had also a positive impact in reducing the light dispersion of the crystals.

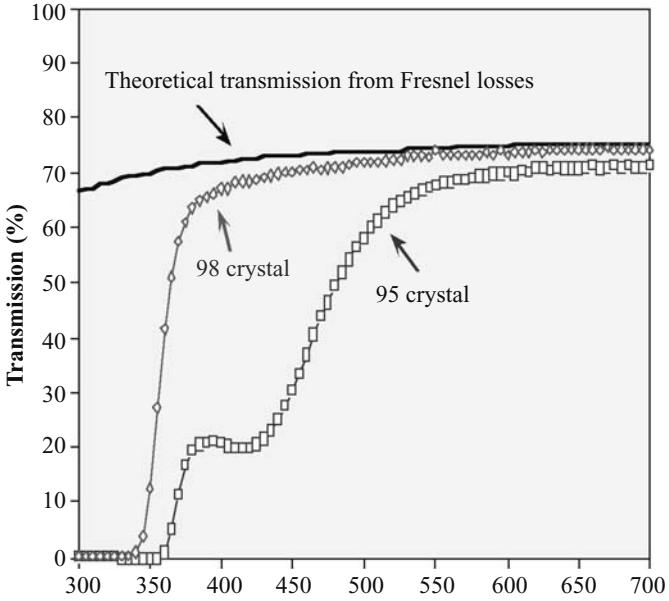

Fig. 6.3. Progress on longitudinal optical transparency of lead tungstate crystals of 23 cm length

6.1.4.3 Origin of Scintillation

Systematic spectroscopic studies carried out on many samples grown in different conditions gave us strong arguments that lead tungstate luminescence is produced by charge transfer transitions in anionic molecular complexes. Both regular WO_4^{2-} and irregular WO_3. tungstate groups are luminescent centers. The WO_4^{2-} blue luminescence (23 800 cm^{-1}) is caused by radiating transitions from triplet levels $^3T_1$, $^3T_2 \rightarrow {}^1A_1$. When an oxygen vacancy appears in a WO_4^{2-}anionic complex the local symmetry of the new WO_3 complex is reduced to C_{3v}. An additional low-symmetry component of the crystalline field splits triplet levels in (A+E) components, producing a shift of the luminescence maximum and causing the green (20 400 cm^{-1}) luminescence at room temperature. Another luminescent center in undoped PWO crystals is associated with the red (15 400 cm^1) luminescence. If the oxygen ion does not escape the crystal but is simply displaced a Frenkel defect is created. This Frenkel defect lowers furthermore the local symmetry of the WO_3 tungsten complex toward a C_3, local symmetry or even lower, thus creating an additional shift and the splitting of the original excited energy terms. Such distorted tungsten anionic complex is responsible for the red luminescence in PWO crystals. In fact, all the mentioned centers contribute to scintillation. However the regular anionic complex blue luminescence is the dominating one

at room temperature for crystals grown in optimal conditions, with specified raw material and appropriate doping.

6.1.4.4 Light Yield Temperature Dependence

Lead tungstate is a crystal of the tungstate family which counts several high light yield but slow scintillators and luminophores like $CdWO_4$, $ZnWO_4$ and $CaWO_4$. The reason for the fast decay tgime of lead tungstate is a strong thermal quenching at room temperature, which also results in a relatively low scintillation light yield. The properties of this crystal make $PbWO_4$ a good compromise between cost and performance for high resolution electromagnetic calorimetry at high energy, where a low light yield is not too much a problem. PWO scintillators have a relatively high temperature dependence of the light yield due to the origin of the radiating centres and the strong thermal quenching. The temperature dependence of the light yield around 20°C is −1.98%/°C. It requires a high precision temperature stabilization of the detecting units. For CMS a complex cooling system maintaining the crystal temperature at 18°C ± 0.1°C had to be designed to guarantee the required precision of 0.5% of the calorimeter at high energy.

6.1.4.5 Slow Scintillation Component

An impressive achievement has been the suppression of slow components in the scintillation of $PbWO_4$. It was observed in 1995 that the optimization for a higher light yield had very often the consequence to produce slow components at a few percent level in the crystals. The slow components in the scintillation related to irregular anionic complexes can be easily suppressed in the crystal by a fine tuning of the stoechiometry of the melt during the crystal growth. However another center was discovered, giving rise to slow components in the scintillation in the microsecond range. It is related to a MoO_4^{2-}anion complex, which is a stableelectron trap center. Molybdenum is an impurity associated to Tungsten. Although raw material is cleaned especially from molybdenum before the crystal growth, the molybdenum ion is chemically very close to the tungsten ion and is rather hard to separate at the raw material production level. In order to suppress this slow component contamination we had to specify a molybdenum impurity concentration in the crystal at the level of less than 1 ppm.

6.1.4.6 Improvement of the Crystal Radiation Hardness

A very critical parameter for Lead Tungstate crystals is their ability to survive in the high radiation environment of the Large Hadron Collider (LHC) in the CMS experiment. A very good stability of the light yield over time is requested to achieve a good resolution of the calorimeter. This problem is

difficult to solve, as it implies a perfect simulation of the radiation conditions in the LHC machine, and a very good understanding of the chemistry of defects in this crystal.

All these aspects have been systematically investigated and impressive progress has been made. Through intensive study of the crystals by different methods the majority of the electron and hole centers in PWO have been identified. Lead Tungstate is characterized by very different vapour pressures for the two components of the melt, Lead and Tungsten oxydes. During the growth process, even from perfectly stoechiometric raw material and whatever the technology used, a dominating leakage of lead takes place from the melt leading to the creation of cation vacancies V_c on the lead site in the host. The charge balance in the crystal impose the concomitant creation of oxygen vacancies. Intrinsic defects based on electron/hole capture by anion or cation vacancies with paramagnetic ground state have never been detected in PWO crystals. This indicates that simple centers like F^+ (anion vacancy V_o + e) and O^- (O^{2-} + h) have no energy levels in the forbidden band or are delocalized in the conduction and valence bands. Therefore the only candidates for metastable color centers in irradiated PWO crystals are cation vacancies capturing two holes of the type $O^-V_cO^-$ or oxygen vacancies capturing even amounts of electrons. Such electronic centers are deep and they are filled mostly through tunneling mechanisms. Very shallow characteristic electron centers have been identified by EPR methods whereas deep ones by TSL and other spectroscopic methods. Through several years of R&D we stated that the scintillation mechanism is not damaged in PWO crystals grown in optimized conditions. This property is as a matter of fact the result of a unique combination of the following crystal features: First, the regular anionic tungstate group is stable under ionizing radiation, second, as follows from our measurements, deep color centers in the crystal do not release electrons in the conduction band when they spontaneously decay. Due to these reasons the scintillation kinetics of the regular emitting centres does not depend on the accumulated dose .However some afterglow can be observed and be dependent on irradiation dose rate if the concentration of V_0 based defects or Mo impurity is large enough in the crystal. The observed radiation damage results therefore only from the transmission degradation resulting from the creation of color centres. The suppression of these color centers has been successfully achieved by a compensation of lead deficiency by additional doping with trivalent ions having a stable valence state like Y or La.

The very promising results of the first phase of the R & D program (1996-1998) induced the collaborating Institutes to continue the ISTC program and to further develop the necessary technologies, including the implementation of stringent quality control methods and special automated measuring equipment. This second R&D phase, financially supported on a 50/50 basis by the European Union and CERN-CMS, has led to excellent results and has set the grounds for the mass production phase, in which the quality of the

mass production technologies is being demonstrated on a large scale. This has been also the opportunity to work on several other aspects: reliability of the production, training of the staff, good managerial structure, quality insurance policy, installation of a modern communication system, development of a network of commercial contacts.

We are now (in 2005) in the last phase of this program which has to be completed for the beginning of 2007. In spite of the fact that more than 150 Czochralski ovens are involved in this production, a large effort had to be developed to increase the productivity in order to reach this goal. In order to build a safety margin in the production a specific development has been made to progressively increase the diameter of the ingots from 38 mm to 65 mm and finally 85 mm (Fig. 6.4). However the implementation of this technology still requires efforts to optimize the cutting and mechanical treatment technology of these large diameter ingots.

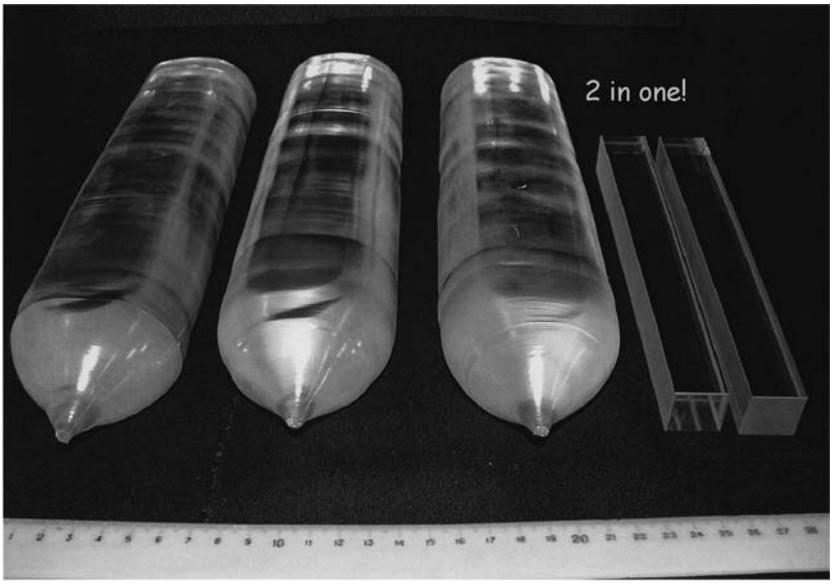

Fig. 6.4. 65 mm ingots with two CMS barrel crystals cut per ingot

6.1.5 Other Experiments Using Lead Tungstate

The large and successful effort placed by CMS on the development of lead tungstate crystals has led several other experiments to choose this crystal for their detector. One can state that lead tungstate has become the most popular scintillation material for HEP applications in the last decade.

The ALICE experiment at CERN is a dedicated heavy-ion experiment at LHC for the study of the initial phase of the collision of heavy nuclei via the direct production of single photons and di-photons. It will also look for signals of chiral-symmetry restoration and jet-quenching as a probe of deconfinement.

The ALICE PHOS calorimeter consists of 17,920 PWO crystals $22 \times 22 \times 180\,\mathrm{mm}^3$ organized in five modules of 3,584 crystals each. Special production facilities have been installed in Apatity, Russia, for the procurement of these crystals grown by the Czochralski method. The detector will be operated at -25°C and read out with avalanche photodiodes [4].

The BTeV experiment at FermiLab is a fixed target experiment to study quark flavor physics, in particular the rare decays of b-flavored particles as the source of CP violation. About 10,000 slightly tapered crystals, with dimensions $(27-28) \times (27-28) \times 220\,\mathrm{mm}^3$ will be assembled in a wall perpendicular to the beam axis. The potential production sites are in Russia and China. The production is expected to take place in the 2006–2008 period [7].

MECO will be installed on the AGS at Brookaven National Laboratory. It is a high sensitivity experiment (2×10^{-17}) which will address rare symmetry-violating process by looking at muons converting to electrons in the field of a nucleus. About 2,300 PWO crystals, with dimensions $30 \times 30 \times 120$ mm^3, will be used for this experiment [8].

The PrimEx experiment at Jefferson Laboratory will use a wall of 1,200 PWO crystals, with dimensions $20.5 \times 20.5 \times 180\,\mathrm{mm}^3$, read out by PMT for a precision measurement of the π° lifetime via the Primakov effect [9].

The photon ball is to be installed into the ANKE magnetic spectrometer at COSY, Jülich. It will study the nucleon structure via the direct measurement of neutral mesons. It is a compact hermetic ball of 876 to 1,100 tapered PWO blocks of 120 mm length read out by the 15 mm quartz light guide and fine mesh Hamamatsu 5505 PMT [10].

The PANDA experiment is a multipurpose detector for the antiproton storage ring at GSI. It will study charmonium, glueball, strangeness, and hypernuclei spectroscopy. The favored technical option so far is based on 7,200 PWO crystals, with dimensions $35 \times 35 \times 150\,\mathrm{mm}^3$, read out by avalanche photodiodes.

6.2 Development of Ce^{3+}-Doped Lutetium-Yttrium Aluminum Perovskite Crystals for Medical Imaging Applications

6.2.1 Introduction

Positron emission tomographs (PET scanners) are more and more recognized as very powerful functional imaging tools in a variety of domains such as basic research in cognitive sciences, clinical oncology, and kinetic pharmaceutical

studies, just to mention a few. Their working principle is based on the reconstruction of the product decay (two γ-rays) of an e^+ labeled tracer injected into the patient. More details are given in Chap. 3. Detection of the two 511 keV gamma rays produced in the electron–positron annihilation allows the in vivo reconstruction of the three-dimensional distribution of the isotope in the body. The detection of the two gamma rays in coincidence requires the use of scintillation detectors. Scintillators used in PET must be dense to optimize detection efficiency, fast to limit number of random coincidences, and have sufficient energy resolution to reject scattered coincidences. State-of-the-art commercial PET scanners are usually based on BGO detector blocks which have a good detection efficiency, but are quite slow (scintillation decay constant 300 ns). Consequently, these scanners operate at a sensitivity of about 1,000 kcps/μCi/ml with a coincidence time window of about 10 ns and a scatter fraction above 30–45%. Next-generation PET scanners need faster scintillators as well as depth-of-interaction encoding, which can be provided by the combination of scintillators with similar density and light yield but different decay time or emission wavelength. This demand has triggered a large effort worldwide in the last decade to explore a variety of crystals for this application.

Lutetium complex structure compounds have rapidly emerged as a natural choice because of the high atomic weight of the lutetium ion, of the good scintillation properties of other rare-earth-based materials such as YAP:Ce and GSO:Ce, and of the possibility of creating a variety of high density crystalline compounds using different ligands. A number of lutetium oxide scintillators doped with trivalent Ce ions have recently been developed, including lutetium orthosilicate LSO (Lu_2SiO_5) [11], lutetium orthophosphate LOP ($LuPO_4$:Ce) [12], lutetium aluminum garnet LuAG ($Lu_3Al_5O_{12}$:Ce) [13, 14], lutetium aluminum perovskite LuAP ($LuAlO_3$:Ce) [15–17], and lutetium pyrosilicate LPS ($Lu_2Si_2O_7$) [18]. These materials tend to exhibit three qualities most desired for gamma detection scintillators: high density and effective atomic number, high scintillation light yield, and short decay time. Although all these crystals have been under investigation for about one decade, only LSO has become a widely used commercially available scintillator so far. Among the others LuAP seems to be the most promising scintillator, with the highest density and the fastest light emission, which make it quite attractive as a gamma detection material. Its density of 8.34 g cm^{-3} is higher than that of LSO (7.34 g cm^{-3}), LuAG (6.9 g cm^{-3}), LPS (6.23 g cm^{-3}), or LOP (6.2 g cm^{-3}). Its attenuation length and photoelectric interaction fraction for 511 keV gamma rays are 1.1 cm and 32%, respectively. It is not hygroscopic and mechanically hard (8.5 Mho), free of cleavage planes, and is therefore relatively easy to cut and polish. Its melting point is below 2,000°C and close to that of LOP (1,947°C) and significantly lower than that of LSO (2,150°C). This is a significant advantage as it can be grown in molybdenum crucibles similar to the well-known $YAlO_3$ (YAP) [19–22]. However, the

growth of this crystal is complicated by phase instability problems between the wanted perovskite phase and a garnet, $Lu_3Al_5O_{12}$, and a monoclinic, $Lu_4Al_2O_9$, phase [23] which compete in a very small temperature domain of the phase diagram. Nevertheless several teams and companies are now consistently producing high quality spontaneously seeded large volume LuAP:Ce ingots.

In order to increase the crystal structure stability heavy co-doping with Y has been proposed [24]. The choice of a solid solution of the type $(Lu_{1-x}$-$Y_x)AlO_3$:Ce, was motivated by several reasons. Yttrium aluminum perovskite has a wider stability region in the Y_2O_3-Al_2O_3 phase diagram than LuAP. The Y^{3+} ion radius is very close to the one of lutetium. Both perovskites have close melting points and can easily create a solid solution. The Czochralski production technology of seeded $(Lu_{1-x}$-$Y_x)AlO_3$:Ce large volume ingots with $x = 0.3, 0.5$ is developed through a joint effort of the Bogoroditsk Techno Chemical Plant (BTCP) from Russia and experts of Crystal Clear Collaboration, CERN, Switzerland. The crystals with $x = 0.7$ can also be produced by horizontally oriented crystallization method similar to $YAlO_3$ crystals.

6.2.2 $(Lu_{1-x}$-$Y_x)AlO_3$:Ce Production Technology

$(Lu_{1-x}$-$Y_x)AlO_3$:Ce crystals have been produced by the Czochralski method using modified equipment of the "Crystal 3M" type. A view of the lutetium-yttrium perovskite production line at BTCP is shown in Fig. 6.5.

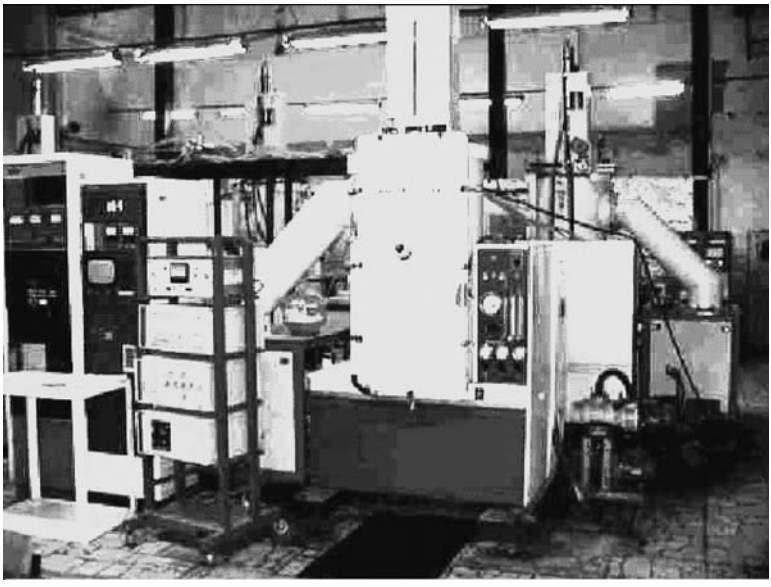

Fig. 6.5. $(Lu_{1-x}$-$Y_x)AlO_3$:Ce crystal production facilities at BTCP

The process of the crystal growth is carried out in an isolated chamber in neutral gas atmosphere. The pulling and rotation speed during the crystal growth can be varied to adjust the ingot diameter at the required value. Before mechanical treatment, the crystal ingots are annealed in low-gradient industrial ovens to reduce the stresses. An open crystallization chamber is shown in Fig. 6.6 with its modernized puller and the induction heating element. A long ingot of the grown $(Lu_{0.7}\text{-}Y_{0.3})AlO_3$:Ce single crystal is also visible.

Crystals of up to 30 mm diameter and 250 mm length with reproducible scintillation parameters have been grown from certified raw materials. Raw material production facilities have been installed which can produce more than 500 kg/year of the specified stoichiometric mixture in powdered form. Tablet compressing machines and preliminary smelting of the raw materials are used to increase the density of the starting material.

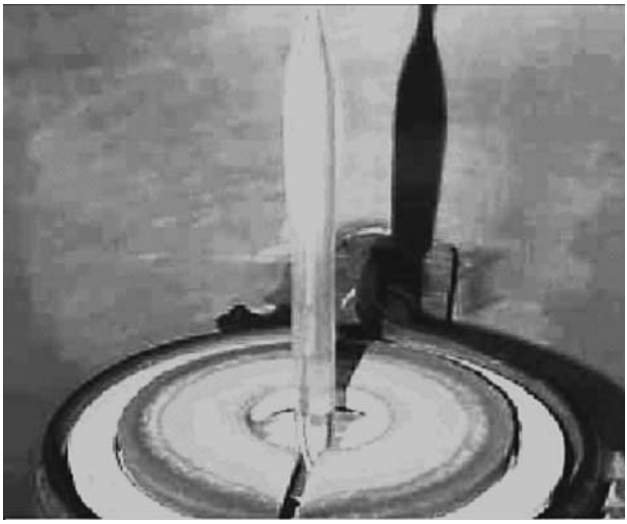

Fig. 6.6. A crystallization chamber with pulled $(Lu_{0.7}\text{-}Y_{0.3})AlO_3$:Ce crystal

More than 500 pixels ($2 \times 2 \times 10\,mm^3$) for the ClearPET® small animal PET scanner [25] can be produced from such an ingot. Work is in progress to progressively increase the ingot diameter up to at least 2 in. The 1 in. diameter scintillation elements for ionizing radiation detectors can be directly produced from the presently grown ingots. One of the scintillation elements cut from a $(Lu_{0.7}\text{-}Y_{0.3})AlO_3$:Ce ingot is shown in Fig. 6.7. LuYAP material is rather hard and not fragile, so standard mechanical treatment technology using diamond powder is applicable.

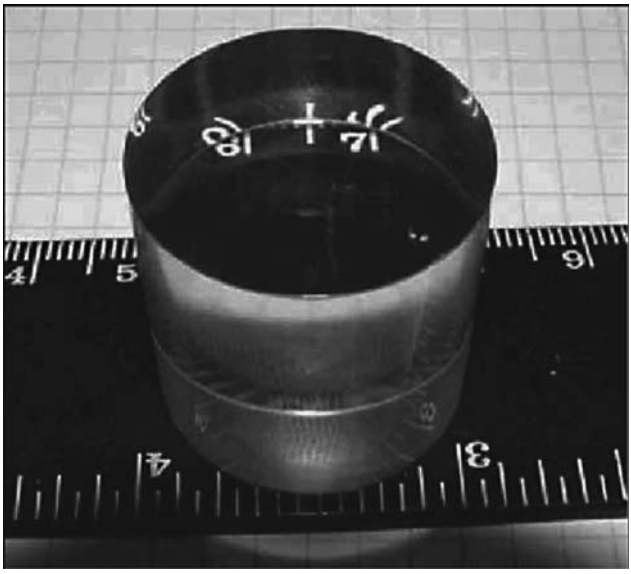

Fig. 6.7. A 1 in $(Lu_{0.7}\text{-}Y_{0.3})AlO_3$:Ce scintillation crystal for spectrometry applications

6.2.3 $(Lu_{1-x}\text{-}Y_x)AlO_3$:Ce Scintillation Properties

The tuning of the Y content in the crystal $(Lu_{1-x}\text{-}Y_x)AlO_3$:Ce allows some flexibility to optimize the optical, chemical, and physical parameters for different applications such as γ-quanta detection, positron emission tomography, and extreme applications such as well logging and hot industrial process control. $(Lu_{1-x}\text{-}Y_x)AlO_3$:Ce crystals have an intermediate position between the well-known $YAlO_3$:Ce and $LuAlO_3$:Ce and their detecting properties, especially density, stopping power, and scintillation kinetics can be adjusted to the specificity of the application. Figures 6.8 and 6.9 show the change of the crystal density and photoelectric linear attenuation coefficient as a function of the Y amount substituted to Lu.

One important aspect of the development strategy for this crystal has been to capitalize on the large amount of efforts made by the CMS collaboration at CERN and at the BTCP plant for the mass production of lead tungstate crystals (see Sect. 6.1). In spite of a tight schedule for the PWO crystals production an intensive R&D program was carried out by the BTCP experts in cooperation with the Crystal Clear Collaboration members with the support of CERN and ISTC.

The first objective was the development of an industrial production chain for the production of crystals with reproducible parameters. For this purpose three different compositions of $(Lu_{1-x}\text{-}Y_x)AlO_3$:Ce with $x = 0.8, 0.5, 0.3$ were selected for the production, starting from the well-known YAP:Ce. The choice

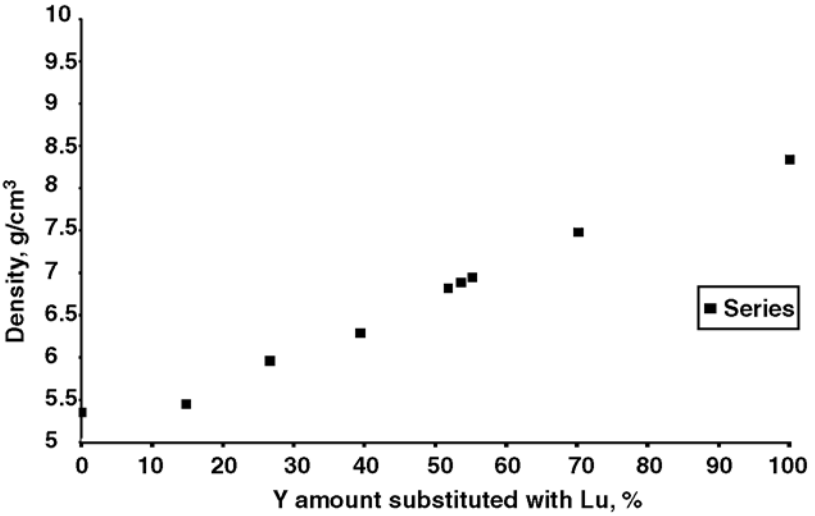

Fig. 6.8. The $(Lu_{1-x}\text{-}Y_x)AlO_3$:Ce crystal density versus the Y amount substituted to Lu

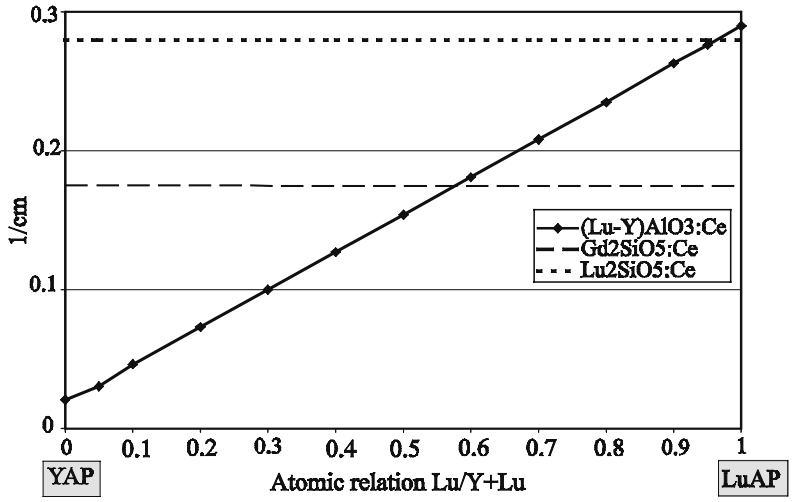

Fig. 6.9. Photoelectric linear attenuation coefficient at 511 keV of $(Lu_x\text{-}Y_{1-x})AlO_3$:Ce as a function of the Lu contents. Values for Lu_2SiO_5:Ce (LSO:Ce) and Gd_2SiO_5:Ce (GSO:Ce) are given for comparison

Table 6.2. Comparison of scintillation and physical properties of $YAlO_3$:Ce and several $(Lu_{1-x}\text{-}Y_x)AlO_3$:Ce crystals

Material	$YAlO_3$:Ce	$(Lu_{0.2}\text{-}Y_{0.8})$ AlO_3:Ce	$(Lu_{0.5}\text{-}Y_{0.5})$ AlO_3:Ce	$(Lu_{0.7}\text{-}Y_{0.3})$ AlO_3:Ce
Density (g cm^{-3})	5.35	5.9	6.5	7.2
λ_{max} emission, (nm)	347	360	375	375
Decay time (fraction in kinetics), ns (%)	30	22 (93) 85 (7)	21 (60) 85 (20) 400 (20)	17 (40) 70 (35) 400 (25)
Light yield (ph MeV^{-1})	16,000	14,000–16,000	12,000–14,000	12,000–14,000
Photoelectric fraction, % at 511 keV	4.4	13.6	22.5	27.1
Attenuation length, cm at 511 keV	2.16	1.88	1.48	1.35

was made as a function of the attenuation coefficient for γ-rays (Fig. 6.9) in order to cover different applications. A comparison of their scintillation and physical properties is shown in Table 6.2.

The crystal with 20% of Y substituted to Lu has a light yield, close to the one of YAP:Ce, a fast scintillation with a very small contribution of slow component and a relatively high density very close to 6 g cm^{-3}. It is a good candidate to be used in medical imaging devices for the detection of soft γ-rays.

The crystal with an equal amount of Lu and Y is in the same range of density and photoelectric fraction at 511 keV as GSO:Ce, but with much better mechanical and temperature properties. It is therefore a better alternative to this crystal.

The last crystal with 70% of Lu is a good candidate to be applied in PET scanners together with LSO:Ce as described in Chap. 5. This crystal has been selected for the ClearPET® scanner, a new generation PET scanner for small animals.

More than 9,000 scintillation pixels with dimensions $2 \times 2 \times 10\,mm^3$ were manufactured for the construction of ClearPET® prototypes. These crystals are used in combination with LYSO:Ce crystals in a phoswich configuration in order to allow depth of interaction measurement by identification of the crystals through their different decay times. A good homogeneity of scintillation characteristics of the crystals grown in different ovens was obtained. The mean value of the light yield is 35% relative to NaT(Tl), i.e. about 12,000 photons MeV^{-1}. The light yield of some of the grown crystals is already close to the theoretical limit which is 50% of NaT(Tl) at room temperature. The study of the temperature dependence of the energy resolution of $(Lu_{0.7}\text{-}Y_{0.3})AlO_3$:Ce pixels shows a progressive improvement when the temperature increases from 300 to 350 K. In the same temperature range the

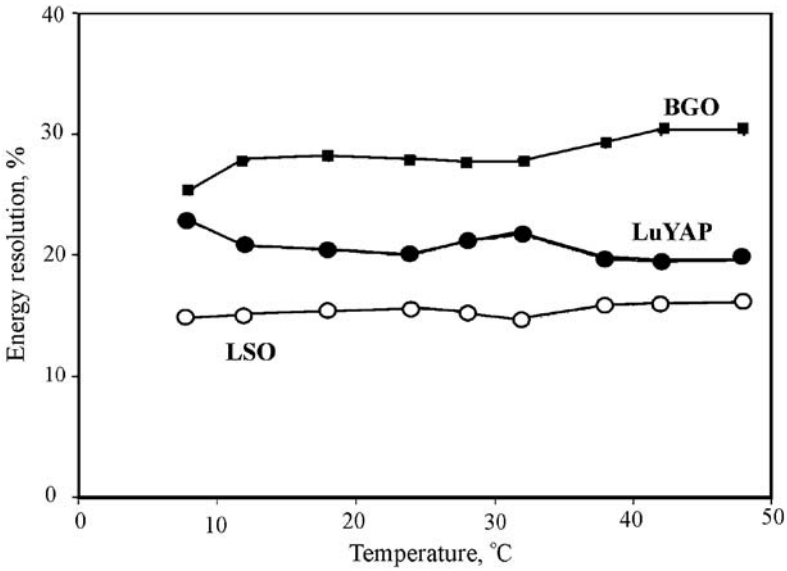

Fig. 6.10. Variation of the energy resolution for 511 keV γ-rays measured with $2 \times 2 \times 10\,\mathrm{mm}^3$ samples of $Lu_{0.7}Y_{0.3}AP$, LSO:Ce, and BGO as a function of temperature (Courtesy of E. Weber and K. Ziemons)

energy resolution of BGO and LSO:Ce degrades [26] as seen in Fig. 6.10. This variation of the energy resolution results from opposite temperature coefficients of the scintillation yield as shown in Fig. 6.11.

The consistency of the crystal quality within the ingot and in particular a small nonuniformity of the light yield and energy resolution along the crystal growth axis are mandatory for an industrial production. The typical variation of the light yield along the crystal growth axis was found to be not more than 5%. It confirms a uniform distribution of the activator along the crystal growth axis. The concentration of the activator in the crystal is well controlled by means of optical absorption spectroscopy. The optical absorption spectrum of the $(Lu_{0.7}\text{-}Y_{0.3})AlO_3$:Ce crystal and its comparison with absorption of the mass produced $YAlO_3$:Ce crystal is shown in Fig. 6.12. As shown in this figure LuYAP still has a large optical absorption in the UV range, extending to the spectral range of the scintillation. This band is attributed to charge transfer transitions $O^{2-} \rightarrow Ce^{4+}$. A large amount of efforts is presently focused on the suppression of this absorption band in the scintillation spectral region, from which one can expect a better light collection uniformity in long pixels and an improved light yield.

The light yield distribution of the grown $(Lu_{0.7}\text{-}Y_{0.3})AlO_3$:Ce crystal ingots produced in the year 2003 is shown in Fig. 6.13. The mean value of the light yield of 1 mm thick plates is 35% of that of NaI(Tl), i.e. about 12,000 photons MeV^{-1}. Some crystals had lower light yield due to macrodefects in-

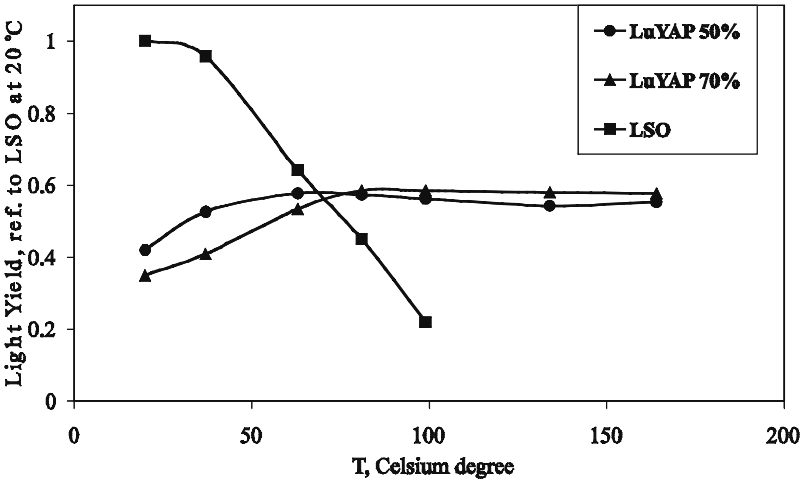

Fig. 6.11. Temperature dependence of LuYAP and LSO light yield

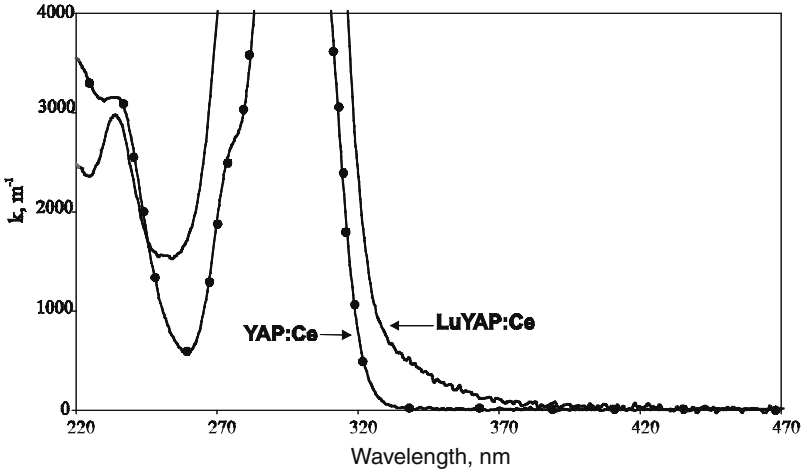

Fig. 6.12. Comparison of the optical absorption of the $(Lu_{0.7}\text{-}Y_{0.3})AlO_3$:Ce and $YAlO_3$:Ce crystals in the region of the first allowed $f \rightarrow d$ transition of the Ce^{3+} ion at 300 K

side the crystals. They were usually cut from bad quality ingots grown after several crystallization cycles in which light scattering centers such as twins and gas bubbles were clearly visible.

The scintillation decay of the grown $(Lu_{0.7}\text{-}Y_{0.3})AlO_3$:Ce crystals can be fitted by three-exponential components with the following time constants and normalized amplitudes: 17 ns—86%, 70 ns—12%, 400 ns—2%. The scintillation pulse shape of crystals with crystallization numbers ranging from 4 to 11 is shown in Fig. 6.14 and compared to LSO:Ce. The crystallization numbers

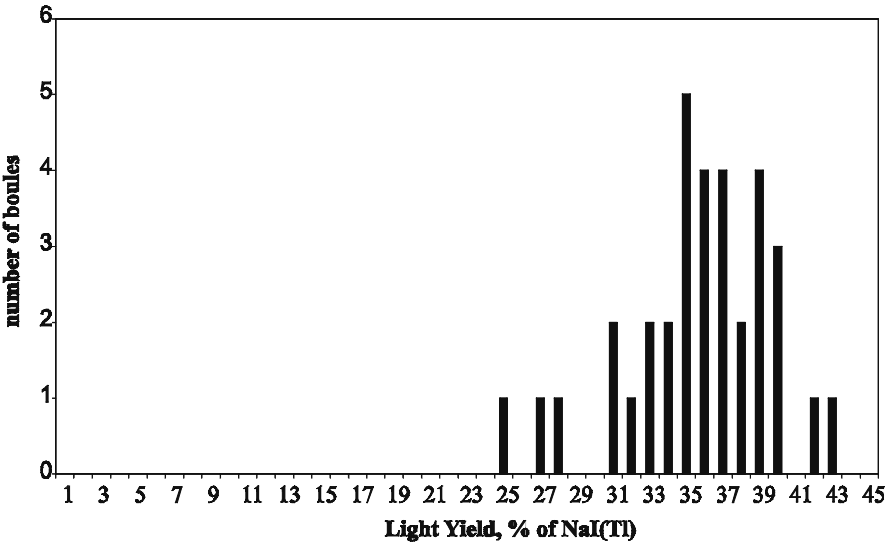

Fig. 6.13. Light yield distribution of $(Lu_{0.7}\text{-}Y_{0.3})AlO_3$:Ce crystals. The light yield of samples cut from the top part of the ingots with thickness 1 mm is compared with $\emptyset 25 \times 1\,mm^3$ NaI(Tl) detector as reference at 300 K

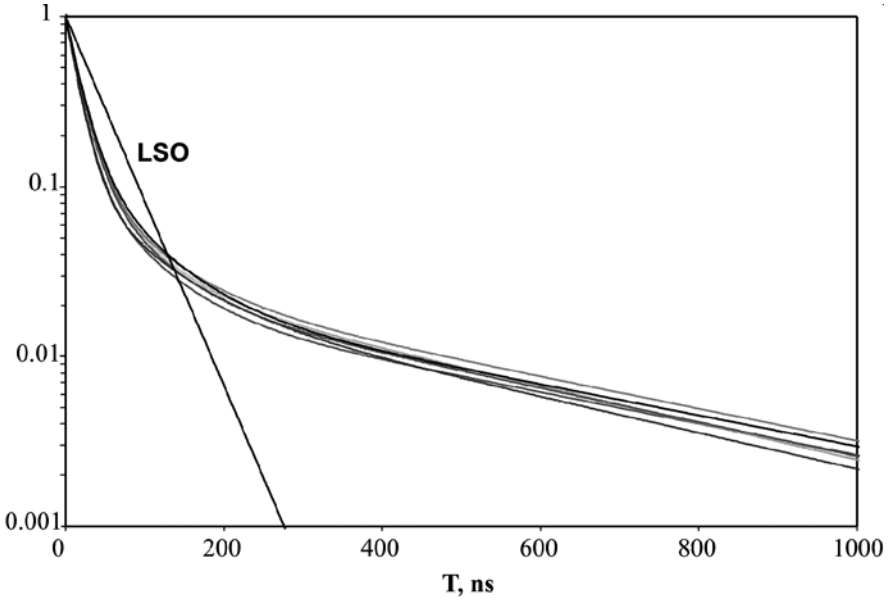

Fig. 6.14. Shape of the $(Lu_{0.7}\text{-}Y_{0.3})AlO_3$:Ce scintillation pulse for crystallization numbers 4–11 compared to that of LSO:Ce at 300 K

are not indicated since there is no correlation between the scintillation pulse shape and the crystallization number. However, for crystallization numbers lower than 3 and greater than 13 some increase of the slow decay component was observed.

The stability of the shape of the LuYAP scintillation pulse and the rather narrow light yield distribution of the grown ingots testify the good quality of raw materials and the reproducibility of the growing process. Effective LSO/LuYAP pulse shape discrimination can be realized on the basis of either the fast or the slow decay component of $(Lu_{0.7}\text{-}Y_{0.3})AlO_3$:Ce.

The influence of the additional optical absorption band on the light collection in $(Lu_{0.7}\text{-}Y_{0.3})AlO_3$:Ce pixels is estimated through the measurement of the light yield of standard $2 \times 2 \times 10\,\text{mm}^3$ pixels in vertical and horizontal positions. Figure 6.15 represents the pulse height spectrum of a Na-22 source measured when the $2 \times 10\,\text{mm}^2$ or the $2 \times 2\,\text{mm}^2$ pixel surface is coupled to the PMT window ("horizontal" and "vertical" geometry). The light yield ratio obtained for LuYAP pixel from these spectra is a good estimator of this absorption band intensity. The ratio LY_{hor}/LY_{vert} is about 2.2 for LuYAP to be compared to 1.85 for LSO pixels as a direct result of a better optical transparency of the LSO crystal in its emission region.

The width of the light yield distribution of $(Lu_{0.7}\text{-}Y_{0.3})AlO_3$:Ce pixels was found to be very close to that of LuYAP boules used for pixel production. The typical light yield distribution of $2 \times 2 \times 10\,\text{mm}^3$ pixels of LuYAP is shown in Fig. 6.16. A subset of 100 samples was randomly taken from a batch of 1,500 pixels. Each pixel was wrapped in two layers of TYVEK reflecting material and the $2 \times 2\,\text{mm}^2$ pixel surface was coupled to the PMT window with Dow Corning Q2-3067 optical grease. A $2 \times 2 \times 10\,\text{mm}^3$ LSO pixel was used as a reference with the same conditions of wrapping and coupling.

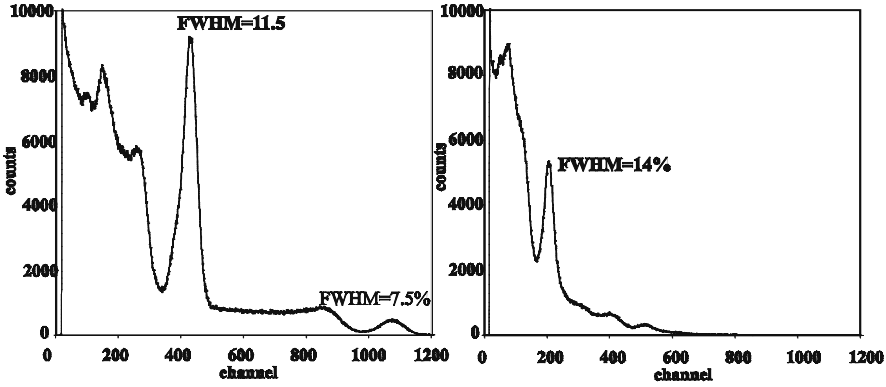

Fig. 6.15. The pulse height spectrum of a Na-22 source measured with the $2 \times 2 \times 10\,\text{mm}^3$ LuYAP pixel. The surface coupled to the PMT window is $2 \times 10\,\text{mm}$ (*left*) and $2 \times 2\,\text{mm}$ (*right*)

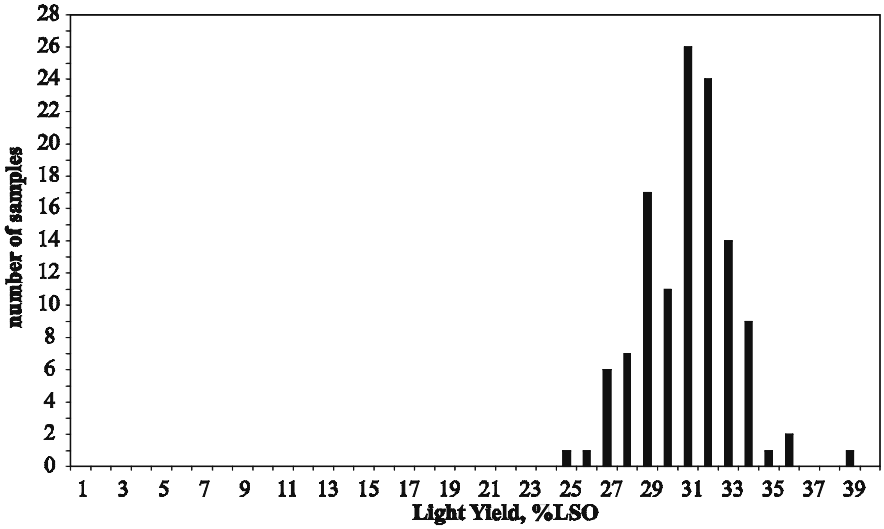

Fig. 6.16. Light yield distribution of $2 \times 2 \times 10\,\mathrm{mm}^3$ pixels of $(Lu_{0.7}\text{-}Y_{0.3})AlO_3$:Ce

After several years of academic work to understand the basic properties of $(Lu_{1-x}\text{-}Y_x)AlO_3$:Ce, impressive progress on the industrial development of this crystal has been made which makes it a very serious candidate for several applications in the low γ-quanta energy registration domain, and particularly medical imaging devices (because of its excellent linearity at low energy and good resulting energy resolution) and well-oil logging (because of its very good properties at high temperature). Moreover, a large potential of improvement exists in light yield and energy resolution through the suppression of the absorption band tail at 360 nm, as well as in decay time when the traps responsible for the slow components will be identified and suppressed.

Besides the $PbWO_4$ scintillator development and industrial implementation, the case of LuYAP:Ce has been another good example in the recent years showing how fundamental research can drive well-organized multidisciplinary collaborations of experts to develop products of high value for the society.

References

1. R&D Proposal for the study of new fast and radiation hard scintillators for calorimetry at LHC: Crystal Clear Collaboration, CERN/DRDC P27/91-15, project RD-18
2. Adeva B, Aguilar-Benitez M, Akbari H et al. (1990) The construction of the L3 experiment. Nucl. Instrum. Methods Phys. Res. A 289: 35–100
3. CMS Technical Proposal, CERN/LHCC 94-38, December 1994
4. ALICE Collaboration Technical Proposal, CERN/LHCC/95-71
5. ISTC: International Science and Technology Center. www.istc.ru

6. Annenkov A, Auffray E, Borisevich A et al. (1999) Suppression of the radiation damage in lead tungstate scintillation crystal. Nucl. Instrum. Methods Phys. Res. A 426: 486–490
7. The BteV proposal, March 2002, BteV-doc-316
8. MECO Collaboration (1999) A proposal to the National Science Foundation to construct the MECO and KORPIO experiments http://meco.ps.uci.edu
9. PrimEx Conceptual Design Report. A precision measurement of the neutral pion lifetime via the Primakof effect. Jefferson Lab, March 3, 2000
10. Barsov S, Bechstedt U, Bothe W et al. (2001) ANKE, a new facility for medium energy hadron physics at COSY-Jülich. Nucl. Instrum. Methods Phys. Res. A 462: 364–381
11. Melcher CL, Schweitzer JS (1992) Cerium-doped lutetium orthosilicate: a fast, efficient new scintillator. IEEE Trans. Nucl. Sci. 39: 502–505
12. Lempicki A, Berman E, Wojtowicz AJ et al. (1993) Cerium-doped orthophosphates: new promising scintillators. IEEE Trans. Nucl. Sci. 40: 384–387
13. Van Eijk CWE, Andriessen J, Dorenbos P et al. (1994) Ce^{3+} doped inorganic scintillators. IEEE Trans. Nucl. Sci. A 348: 546–550
14. Ryskin NN, Dorenbos P, Van Eijk CWE et al. (1994) Scintillation properties of $Lu_3Al_{5-x}Sc_xO_{12}$ crystals. J. Phys.: Condens. Matter 6: 10423–10434
15. Moses WW, Derenzo SE, Fyodorov A et al. (1995) $LuAlO_3$:Ce—a high density, high speed scintillator for gamma detection. IEEE Trans. Nucl. Sci. 42: 275–279
16. Minkov BI (1994) Promising new lutetium based single crystals for fast scintillators. Funct. Mater. 1: 103–105
17. Lempicki A, Randles MH, Wisniewski D et al. (1995) $LuAlO_3$:Ce and other aluminate scintillators. IEEE Trans. Nucl. Sci. 42: 280–284
18. Pauwels D, Le Masson N, Viana B et al. (2000) A novel inorganic scintillator: $Lu_2Si_2O_7$:Ce^{3+} (LPS). IEEE Trans. Nucl. Sci. 47: 1787–1790
19. Weber MJ (1973) Optical spectra of Ce^{3+} sensitized fluorescence in $YAlO_3$. J. Appl. Phys. 44: 3205–3208
20. Autrata R, Schouer P, Kvapil Jiri et al. (1983) A single crystal of $YAlO_3$:Ce^{3+} as fast scintillator in SEM. Scanning 5: 91–96
21. Baryshevsky VG, Korzhik MV, Moroz VI et al.(1991) $YAlO_3$:Ce—fast-acting scintillators for detection of ionizing radiation. Nucl. Instrum. Methods Phys. Res. B 58: 291–293
22. Korzhik MV, Misevich OV, Fyodorov AA (1999) $YAlO_3$:Ce scintillators: application for X- and soft γ-ray detection. Nucl. Instrum. Methods Phys. Res. B 72: 499–501.
23. Smirnova SA, Korzhik MV (1996) Growth of crystals yttrium-aluminum perovskites with rare earth elements. In: Dorenbos P, van Eijk CWE (Eds). Proc. Int. Conf. on Inorganic Scintillators and Their Applications, SCINT'95. Delft University Press, The Netherlands, pp 495–497
24. Trower WP, Korzhik MV, Fedorov AA et al. (1996) Cerium doped luthetium-based single crystal scintillator. In: Dorenbos P, van Eijk CWE (Eds). Proc. Int. Conf. on Inorganic Scintillators and Their Applications, SCINT'95. Delft University Press, The Netherlands, pp 355–358
25. A PET scanner. Patent WO03/001242A1
26. Weber S, Christ D, Kurzeja M et al. (2003) Comparison of LuYAP, LSO, and BGO as scintillators for high resolution PET detectors. IEEE Trans. Nucl. Sci. 50: 1370–1372